

Efficient Electric Vehicle Charging Allocation: A Two-Stage Optimization and Participation Analysis *

LIU Ruiwu & ZHU Yangjian

Abstract

Electric vehicles (EVs) require substantially longer refueling times than gasoline vehicles, which can generate severe congestion at charging stations when demand concentrates. We propose a two-stage allocation framework for EV charging networks. In Stage 1, a central coordinator determines station-level admission quotas to control worst-station delay using a queue-informed congestion metric. In Stage 2, given these quotas and feasibility constraints (e.g., reachability), the coordinator solves a utility-maximizing capacitated assignment to allocate EVs across stations. To keep Stage 2 tractable while capturing heterogeneous charging needs, we pre-compute each EV–station pair’s optimal charging amount in closed form under a battery-capacity constraint and then solve a transportation/assignment problem. Finally, we introduce a reduced-form participation model to characterize adoption thresholds under network benefits, spillovers, and coordination costs. Numerical experiments illustrate substantial reductions in worst-case congestion with limited impact on average utility, and highlight scaling patterns as the number of stations increases.

Keywords: EV charging allocation; queueing; congestion control; transportation/assignment; network externalities; participation threshold.

1 Introduction

EV adoption has increased rapidly in many regions, while charging infrastructure expansion often lags behind. Unlike gasoline refueling, EV charging can take tens of minutes or longer, so demand concentration can cause long queues and extreme waiting times at popular stations. Uncoordinated charging decisions also create congestion externalities: an EV choosing a station increases delays for others, while underutilized stations remain idle.

A large literature studies EV charging using queueing models, dynamic pricing, routing algorithms, and game-theoretic approaches (e.g., Stackelberg-type interactions and matching-based formulations). In addition, participation issues arise when coordination requires users to share information or comply with platform recommendations. Similar to

*This manuscript is a highly preliminary draft. Both the model and the simulation design will be extended in future versions. For readability, we adopt the simplest formulations and descriptions that convey the main ideas.

coalition-formation problems in International Environmental Agreement (IEA) analysis, nonparticipants may still benefit from spillovers created by a coordinated subgroup, which generates free-riding incentives and adoption thresholds.

Contributions Our paper contributes to the EV charging allocation literature along several dimensions. First, while much of the existing work studies either congestion using queueing models or allocation using pricing/routing/matching mechanisms, we provide a unified two-stage framework that explicitly separates *system-level congestion control* from *user-level welfare maximization*. Stage 1 introduces station-level admission quotas that directly target tail congestion by minimizing the worst-station delay, thereby internalizing congestion externalities at the system level. This contrasts with approaches that focus on individual best responses (e.g., uncoordinated routing) or primarily improve average performance without explicitly controlling worst-case congestion.

Second, relative to stable-matching-based scheduling (e.g., Gale–Shapley-type mechanisms used in prior EV charging applications), our Stage 2 allocation is formulated as a welfare-maximizing capacitated assignment under quotas. This reflects the practical reality that stations typically do not “reject” customers in the way matching models allow, and it yields a directly implementable allocation rule. To keep the model tractable while incorporating heterogeneous charging needs, we precompute each EV–station pair’s optimal charging amount in closed form under a battery-capacity constraint, reducing Stage 2 to a transportation/assignment problem.

Third, our formulation clarifies two economically meaningful ways of accounting for congestion in welfare. When $\eta = 0$, congestion is internalized indirectly through the quota constraints (a hard congestion-control layer); when $\eta > 0$, congestion is priced into welfare as an explicit time-cost term (a soft adjustment). This provides a clean bridge between operational constraints and welfare interpretation that is often implicit in the existing literature.

Finally, beyond operational allocation, we study voluntary participation using a reduced-form adoption model motivated by network externalities and coalition stability. Unlike most scheduling papers that assume full participation, our participation module characterizes adoption thresholds in the presence of spillovers (free-riding) and coordination costs, highlighting when a coordinated platform is sustainable and why “cold-start” incentives may be required.

Paper organization. Section 2 introduces the two-stage model. Section 3 presents numerical experiments and simulation results. Section 4 presents the participation model. Section 5 discusses limitations and extensions, and Section 6 concludes.

2 Model

2.1 Time, sets, and notation

Time is discrete, indexed by $k = 0, 1, 2, \dots$, with scheduling interval length $T > 0$. (For notational simplicity, one may normalize $T = 1$; then rates such as μ_i are measured per interval.)

Let $\mathcal{S} = \{1, \dots, S\}$ be the set of charging stations (CSs), indexed by $i \in \mathcal{S}$. In each interval k , a set of EVs $\mathcal{N}(k)$ arrives, with $N(k) = |\mathcal{N}(k)|$ and $\gamma(k) \equiv N(k)$ ($\gamma(k)$ denotes the exogenous inflow of new charging requests at epoch k).

Station i has: (i) $c_i \in \mathbb{Z}_+$ chargers; (ii) per-charger service rate $\mu_i > 0$; (iii) unit price $p_i \geq 0$ (extensions allow $p_i(k)$). Each EV $n \in \mathcal{N}(k)$ has $SoC_n(k) \in [0, 1]$, distance $d_{ni} \geq 0$ to station i , and willingness-to-pay cap $p_n^{\max} \geq 0$. Let $\kappa > 0$ be a range conversion parameter (distance per unit SoC). The feasible station set for EV n is

$$\mathcal{S}_n(k) = \{i \in \mathcal{S} : d_{ni} \leq \kappa \cdot SoC_n(k)\}. \quad (1)$$

We assume $\mathcal{S}_n(k) \neq \emptyset$ for all n (otherwise a fallback rule applies). For example, $d_{ni} \leq \kappa SoC_n(k)$ means EV n can reach station i if its remaining charge supports the travel distance.

2.2 Stage 1: flow–queue coupling and congestion control

State and flow variables. Let $x_i(k) \geq 0$ denote the number of EVs *in station i* at the beginning of interval k (waiting + in service). Let $f_i(k) \geq 0$ be the number of EVs admitted/routed to station i during interval k (vehicles per interval), and $g_i(k) \geq 0$ the number departing station i during interval k (vehicles per interval). The station queue evolves as

$$x_i(k+1) = x_i(k) + f_i(k) - g_i(k), \quad \forall i \in \mathcal{S}. \quad (2)$$

Flow conservation is

$$\sum_{i \in \mathcal{S}} f_i(k) = \gamma(k), \quad f_i(k) \geq 0. \quad (3)$$

Arrival-rate estimation via historical smoothing (moving average). We distinguish per-interval counts $f_i(k)$ from the continuous-time arrival rate $\lambda_i(k)$ used in queueing performance. We estimate

$$\lambda_i(k) = \frac{1}{H} \sum_{\ell=0}^{H-1} f_i(k-\ell), \quad H \in \mathbb{Z}_+, \forall i \in \mathcal{S}. \quad (4)$$

(Note that $f_i(k)$ enters $\lambda_i(k)$ through the moving-average estimator, so Stage 1 has a short-memory effect over H epochs.) For early intervals $k < H$, one may use a shorter window or initialize $f_i(k) = 0$ for $k < 0$.

2.2.1 Queueing background (M/M/ c_i) and a tractable output approximation

Within each interval, station i is approximated as an M/M/ c_i queue with arrival rate $\lambda_i(k)$ and per-server service rate μ_i . Define offered load and utilization:

$$\rho_i(k) = \frac{\lambda_i(k)}{\mu_i}, \quad v_i(k) = \frac{\lambda_i(k)}{c_i \mu_i} = \frac{\rho_i(k)}{c_i}. \quad (5)$$

Stability requires

$$\lambda_i(k) < c_i \mu_i, \quad \forall i, k. \quad (6)$$

Let $P_{0,i}(k)$ denote the probability that station i is empty in steady state. Then

$$P_{0,i}(k) = \left[\sum_{n=0}^{c_i-1} \frac{\rho_i(k)^n}{n!} + \frac{\rho_i(k)^{c_i}}{c_i! \left(1 - \frac{\rho_i(k)}{c_i}\right)} \right]^{-1}. \quad (7)$$

The expected number of EVs *in station i* (waiting + in service) admits the standard Erlang-C form

$$\mathbb{E}[x_i | \lambda_i(k)] = \frac{\rho_i(k)^{c_i+1}}{c_i c_i! \left(1 - \frac{\rho_i(k)}{c_i}\right)^2} P_{0,i}(k) + \rho_i(k). \quad (8)$$

Standard Erlang-C formulas map $\lambda_i(k)$ to $\mathbb{E}[x_i | \lambda_i(k)]$ (via $P_{0,i}(k)$, etc.). (While the Erlang-C expressions provide a standard steady-state mapping from $\lambda_i(k)$ to expected congestion, our Stage 1 implementation relies on the explicit dynamic closure (9)–(10) to update $(x_i(k), W_i(k))$ epoch-by-epoch in simulation and optimization.) However, for dynamic updates (2) we require an explicit outflow function g_i as a function of the state $x_i(k)$. Inverting the steady-state mapping to obtain $g_i = g_i(x_i)$ in closed form is generally intractable for $c_i > 1$. Following the tractable approximation approach in Gusrialdi et al. (2017) (and related distributed queue-control work), we close the dynamics using an explicit saturating outflow map:

$$\hat{g}_i(x) = c_i \mu_i \frac{x}{1+x}, \quad x \geq 0, \quad (9)$$

so departures per interval are

$$g_i(k) = \hat{g}_i(x_i(k)) = c_i \mu_i \frac{x_i(k)}{1+x_i(k)}. \quad (10)$$

Delay metric (Little’s law). Because $x_i(k)$ counts EVs in station i (waiting + in service), Little’s law implies that the expected *time in system* (sojourn time) is

$$W_i(k) = \frac{x_i(k)}{\lambda_i(k)}. \quad (11)$$

(Optionally, queueing delay can be defined as $W_{q,i}(k) = W_i(k) - 1/\mu_i$.)

2.2.2 Stage 1 optimization and numerical solution

Stage 1 chooses admissions $\{f_i(k)\}$ to reduce worst-station delay. Introducing an auxiliary variable z yields the epigraph form (equivalent to):

$$\min_{\{f_i(k)\}, z} z \quad (12)$$

$$\text{s.t. } W_i(k) \leq z, \quad \forall i \in \mathcal{S}, \quad (13)$$

$$\sum_{i \in \mathcal{S}} f_i(k) = \gamma(k), \quad f_i(k) \geq 0, \quad \forall i, \quad (14)$$

$$\lambda_i(k) \text{ is given by (4),} \quad \forall i, \quad (15)$$

$$\lambda_i(k) < c_i \mu_i, \quad \forall i. \quad (16)$$

The state evolves by (2)–(10). Problem (12)–(16) can be solved numerically at each epoch using a standard nonlinear solver. Alternatively, one may biselect on z and check feasibility; feasibility is monotone in z .

2.3 Stage 2: utility-maximizing assignment under Stage-1 quotas

Binary assignment decision. Let $x_{ni}(k) \in \{0, 1\}$ indicate whether EV n is assigned to station i in interval k . Feasibility requires $x_{ni}(k) = 0$ for all $i \notin \mathcal{S}_n(k)$. Each EV is assigned to exactly one feasible station:

$$\sum_{i \in \mathcal{S}_n(k)} x_{ni}(k) = 1, \quad \forall n \in \mathcal{N}(k). \quad (17)$$

Stage 1 admissions $f_i(k)$ act as station quotas:

$$\sum_{n \in \mathcal{N}(k)} x_{ni}(k) \leq f_i(k), \quad \forall i \in \mathcal{S}. \quad (18)$$

Charging amount: precomputed optimal $E_{ni}^*(k)$. Let $E_{ni}(k)$ denote the energy fraction charged by EV n if it uses station i in interval k . Battery-capacity constraint:

$$0 \leq E_{ni}(k) \leq 1 - SoC_n(k). \quad (19)$$

We capture heterogeneity in charging preference via a curvature/anxiety parameter. Each EV has a baseline $\bar{s}_n > 0$ and we allow state dependence:

$$S_n(k) = \bar{s}_n(1 + \alpha(1 - SoC_n(k))), \quad \alpha \geq 0. \quad (20)$$

Define the charging benefit function for pair (n, i) :

$$\phi_{ni}(E) = -\frac{1}{2}S_n(k)E^2 + (p_n^{\max} - p_i)E. \quad (21)$$

For fixed (n, i) , solve the one-dimensional concave problem

$$E_{ni}^*(k) = \arg \max_{0 \leq E \leq 1 - SoC_n(k)} \phi_{ni}(E), \quad (22)$$

which admits the closed-form solution:

$$E_{ni}^*(k) = \min \left\{ \max \left\{ \frac{p_n^{\max} - p_i}{S_n(k)}, 0 \right\}, 1 - SoC_n(k) \right\}. \quad (23)$$

Utility and the role of congestion. Let $\tau > 0$ be the distance disutility weight. Optionally, the Stage-1 congestion signal enters welfare via a time-cost weight $\eta \geq 0$. For $i \in \mathcal{S}_n(k)$, define:

$$u_{ni}(k) = \phi_{ni}(E_{ni}^*(k)) - \tau d_{ni} - \eta W_i(k). \quad (24)$$

Setting $\eta = 0$ omits an explicit delay term in Stage 2 (congestion is controlled indirectly via quotas), while $\eta > 0$ yields a fully closed welfare interpretation.

Stage 2 optimization problem. The platform solves the capacitated assignment problem:

$$\max_{\{x_{ni}(k)\}} \sum_{n \in \mathcal{N}(k)} \sum_{i \in \mathcal{S}_n(k)} u_{ni}(k) x_{ni}(k) \quad (25)$$

$$\text{s.t.} \quad \sum_{i \in \mathcal{S}_n(k)} x_{ni}(k) = 1, \quad \forall n \in \mathcal{N}(k), \quad (26)$$

$$\sum_{n \in \mathcal{N}(k)} x_{ni}(k) \leq f_i(k), \quad \forall i \in \mathcal{S}, \quad (27)$$

$$x_{ni}(k) \in \{0, 1\}, \quad \forall n, i. \quad (28)$$

This is a transportation/assignment problem, directly implementable and simulatable (often solvable efficiently via min-cost flow / LP methods).

3 Numerical Experiments and Simulation Results

We simulate the system in discrete epochs. In each epoch, new EV requests arrive, the platform determines station quotas (Stage 1), and then assigns EVs under quotas (Stage 2). For baseline comparison, we also consider a free-choice strategy in which EVs select the nearest feasible station, and a matching-based baseline (Yoshihara/Gale–Shapley) when applicable.

3.1 Simulation design

Time resolution and arrivals. We simulate the system over discrete decision epochs. At each epoch k , a batch of new EV charging requests arrives. The number of new requests $\gamma(k)$ is generated by a Poisson distribution with parameter Λ (e.g., $\Lambda = 30$). All arriving EVs are assumed to require charging.

Cold start and per-epoch sequence. Stage 1 uses the smoothed arrival-rate estimator (moving average) to compute $\lambda_i(k)$, which requires past inflow data. Therefore, we adopt the following initialization: (i) in the first epoch, quotas $\{f_i(1)\}$ are allocated proportionally to incoming demand (e.g., proportional to station capacity); (ii) only the Stage 2 allocation is solved in the first epoch; (iii) from the second epoch onward, we solve Stage 1 to determine quotas, and then solve Stage 2 under these quotas.

More precisely, for each epoch $k \geq 2$:

1. Observe the station states $\{x_i(k)\}$ and new arrivals $\mathcal{N}(k)$ with total size $\gamma(k)$.
2. **Stage 1 (quota control):** solve the min–max congestion problem to obtain station quotas $\{f_i(k)\}$.
3. Update smoothed arrival-rate estimates $\lambda_i(k)$ and compute departures using the explicit saturating outflow approximation; update queue states via $x_i(k+1) = x_i(k) + f_i(k) - g_i(k)$.

4. **Stage 2 (assignment):** compute each feasible EV–station pair’s utility (including the closed-form optimal charging amount), and solve the capacitated assignment problem under quotas.

Baselines. We compare our two-stage mechanism with:

- **Free choice (nearest-station) baseline:** each EV selects the nearest feasible station.
- **Matching-based baseline (Yoshihara/Gale–Shapley):** the algorithm proposed in Yoshihara et al. (2020), under the same environment configuration (when applicable).

3.2 Parameter setting

Tables 1–3 summarize the core parameters used for EVs and charging stations.

Class	Parameter	Description
EV	$SoC_n(k)$	State of charge (normalized to $[0, 1]$)
EV	p_n^{\max}	Willingness-to-pay cap
EV	\bar{s}_n, α	Curvature/anxiety parameters in (20)
EV	position	Entry location (used to compute d_{ni})
CS	c_i	Number of chargers
CS	μ_i	Service rate per charger
CS	p_i	Price per unit charge
CS	location	Station location
System	Λ	Poisson arrival intensity for $\gamma(k)$
System	H	Moving-average window length for $\lambda_i(k)$

Table 1: Parameter descriptions for EVs and charging stations (core).

CS idx	c_i	location	price
1	2	8	62
2	1	12	60
3	3	20	58

Table 2: Example station configuration.

Parameter	Setting
p_n^{\max}	Randomly assigned (e.g., uniform on $[80, 120]$)
Position	Randomly assigned over a line segment (e.g., $[0, 20]$)
Initial SoC_n	Randomly assigned (e.g., uniform on $[0.1, 0.9]$)
Anxiety type	Randomly assigned via (\bar{s}_n, α)

Table 3: Example EV parameterization.

3.3 Results: free choice vs two-stage optimization

Stage 1 quotas primarily target *extreme congestion* by preventing demand from concentrating on already overloaded stations. Stage 2 then allocates EVs within these quotas to maximize aggregate utility, so the welfare impact of congestion control is moderated.

We observe that worst-case congestion measures (e.g., maximum queue length and time-related metrics) are substantially improved under the two-stage mechanism. At the same time, average utility can remain close to the free-choice baseline in small networks, because limited station options constrain how much utility can be improved purely through assignment. As the number of stations increases, the feasible choice set expands and the utility-maximizing assignment becomes more effective, so the gap in average utility can widen in favor of the optimized allocation (Figure 4).

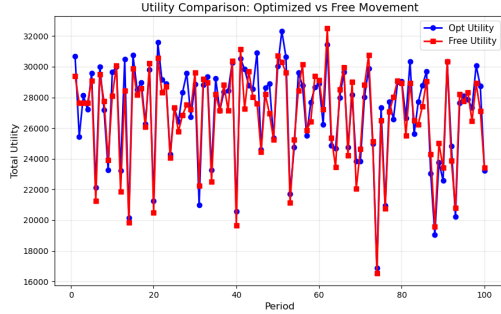


Figure 1: Utility: free vs optimization

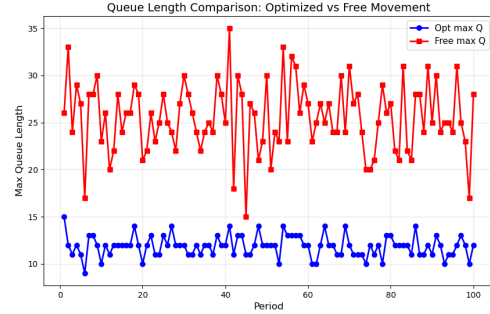


Figure 2: Queue length: free vs optimization

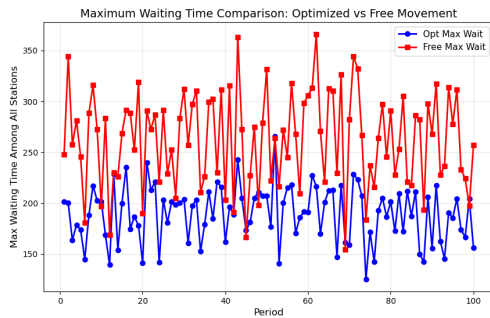


Figure 3: Time saving: free vs optimization

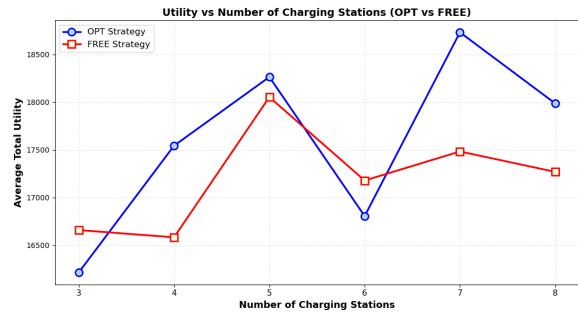


Figure 4: Average utility vs number of stations

Interpreting $\eta = 0$ vs $\eta > 0$ (under construction). When $\eta = 0$, congestion is internalized indirectly through the quota constraints in (18), creating a *hard* congestion-control layer. When $\eta > 0$, congestion enters utility directly as a *soft* welfare adjustment; marginal EVs may be shifted away from more congested stations, potentially further reducing delay at the cost of small utility trade-offs (depending on η). If desired, one can report sensitivity results by varying η while keeping the same baseline settings.

3.4 Comparison with matching-based baseline

We also compare our solution with the allocation algorithm of Yoshihara et al. (2020) under the same environment configuration as in the free-choice comparison. Figures 5–7 summarize the comparison.

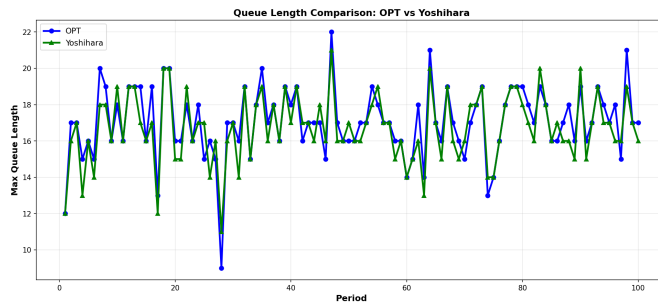


Figure 5: Queue length: Yoshihara's vs optimization

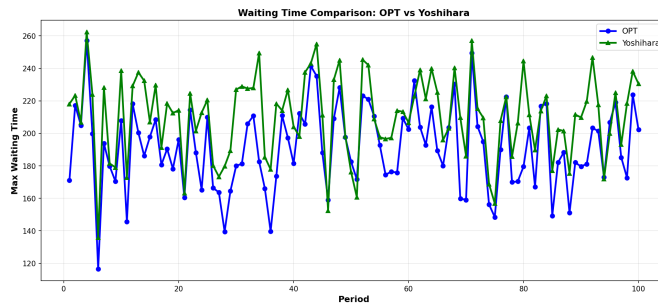


Figure 6: Max delay: Yoshihara's vs optimization

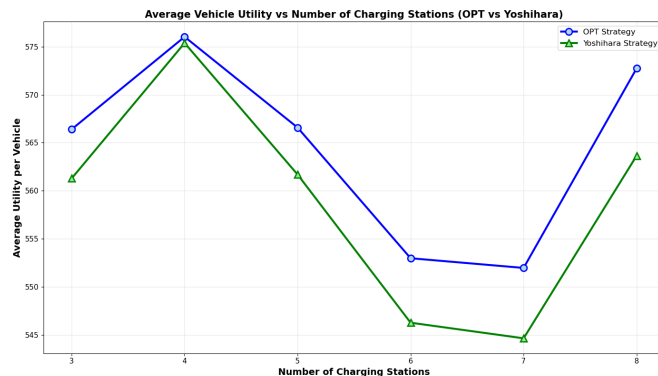


Figure 7: Scaling: average utility vs number of stations

The key difference lies in Stage 2. Our mechanism solves a welfare-maximizing capacitated assignment under Stage 1 quotas and feasibility constraints, without relying on station-side rejection. By contrast, matching-based approaches may incorporate station preferences and rejection behavior, which can affect both allocation efficiency and congestion outcomes. In particular, even when Stage 1-type congestion control is similar, differences in Stage 2 allocation logic can lead to different utility and delay profiles.

4 Participation Decision Analysis

Purpose and link to Stage 1–2. Stages 1–2 characterize how a coordinated platform can (i) control congestion through station-level quotas and (ii) improve allocative efficiency through a capacitated assignment. In this subsection, we introduce a reduced-form participation model to capture the adoption threshold of such a platform. The key parameters summarize the *expected incremental gains from coordination* (as delivered by Stages 1–2), the *spillover benefits to nonparticipants*, and the *coordination/overhead costs* of operating the platform.

4.1 A reduced-form adoption model

Players and participation rate. Consider a large population of EV users. Each user chooses whether to join the coordinated platform (J) or not join (NJ). Let $m \in [0, 1]$ denote the fraction of users who join (participation rate).

Payoffs (reduced form). Let $\pi^J(m)$ and $\pi^{NJ}(m)$ denote the expected utilities of a representative user who joins and does not join, respectively. We model:

$$\pi^J(m) = Am - Bm^2 - c, \quad (29)$$

$$\pi^{NJ}(m) = Gm, \quad (30)$$

where $A > 0$ captures the strength of network benefits from coordination (e.g., better matching and congestion reduction), $G \in [0, A)$ captures spillover benefits enjoyed by nonparticipants (free-riding), $B > 0$ captures convex coordination/overhead or congestion costs increasing with platform scale, and $c \geq 0$ is the (per-user) cost of joining (e.g., registration, privacy, compliance, or fees).

Join condition and sustainable participation interval. A user joins if joining yields at least as much utility as not joining:

$$\pi^J(m) \geq \pi^{NJ}(m) \iff (A - G)m - Bm^2 - c \geq 0. \quad (31)$$

Let $\Delta = (A - G)^2 - 4Bc$. If $\Delta < 0$, inequality (31) has no real interior solution. If $\Delta \geq 0$, define the two roots

$$m_{1,2} = \frac{(A - G) \mp \sqrt{\Delta}}{2B}. \quad (32)$$

Then joining is individually rational for

$$m \in [m_1, m_2] \cap [0, 1]. \quad (33)$$

Interpretation. For small m , network benefits are insufficient to offset the join cost c . For large m , convex overhead/congestion costs Bm^2 dominate. Thus, the platform is sustainable only for intermediate participation rates, consistent with threshold-type adoption and the need for early-stage incentives (e.g., subsidies) to overcome the cold-start problem.

4.2 Optional heterogeneity extension

To reflect user heterogeneity while retaining tractability, one may allow heterogeneous join costs c_n . Then user n joins if $(A - G)m - Bm^2 \geq c_n$. Let $F_C(\cdot)$ denote the CDF of c_n in the population. The participation rate satisfies the fixed-point condition

$$m = F_C((A - G)m - Bm^2), \quad (34)$$

which admits standard threshold dynamics and can be used in numerical experiments if desired. In the main text, we focus on the homogeneous- c benchmark (29)–(30) to highlight the participation threshold mechanism.

5 Discussion

This paper provides a simulation-ready two-stage framework for EV charging allocation that targets worst-case congestion in Stage 1 and preserves welfare in Stage 2 under capacity constraints. The participation module provides a transparent characterization of adoption thresholds and free-riding incentives.

Several limitations remain. First, the queue-control layer relies on a tractable approximation for outflow and a quasi-stationary interpretation within epochs. Second, the reduced-form participation module summarizes Stage 1–2 gains using parameters (A, G, B, c) rather than deriving them endogenously. Third, “cold start” in the first epoch is unavoidable without prior data; our proportional initialization follows the original simulation spirit.

Future work includes calibrating congestion and participation parameters using real charging-network data, introducing time-varying prices and reservation/slot mechanisms, and improving computational efficiency for large-scale deployments.

6 Conclusion

We propose a two-stage optimization framework for EV charging allocation. Stage 1 determines station quotas to control extreme congestion, and Stage 2 solves a utility-maximizing capacitated assignment using closed-form charging amount decisions. We also present a reduced-form participation model that yields adoption thresholds under network benefits, spillovers, and coordination costs. Numerical experiments suggest substantial reductions in worst-case congestion while maintaining competitive average utility.

References

- Gusrialdi, A., Qu, Z., and Simaan, M. A. (2017). Distributed scheduling and cooperative control for charging of electric vehicles at highway service stations. *IEEE Transactions on Intelligent Transportation Systems*, 18(10):2713–2727.
- Yoshihara, M., Hafizulazwan Mohamad Nor, M., Kono, A., Namerikawa, T., and Qu, Z. (2020). Non-cooperative optimization algorithm of charging scheduling for electric vehicle. *SICE Journal of Control, Measurement, and System Integration*, 13(6):265–273.